BIM_{EL}, an intrinsically disordered protein, is degraded by 20S proteasomes in the absence of poly-ubiquitylation

Ceri M. Wiggins[1], Peter Tsvetkov[2], Mark Johnson[1], Claire L. Joyce[1], Christopher A. Lamb[3], Nia J. Bryant[3], David Komander[4], Yosef Shaul[2] and Simon J. Cook[1,*]

[1]Laboratory of Molecular Signalling, The Babraham Institute, Babraham Research Campus, Cambridge, CB22 3AT, UK
[2]Department of Molecular Genetics, Weizmann Institute of Science, Rehovot 76100, Israel
[3]Institute of Molecular, Cell and Systems Biology, College of Medical, Veterinary and Life Sciences, University of Glasgow, Glasgow G12 8QQ, UK
[4]MRC Laboratory of Molecular Biology, Hills Road, Cambridge CB2 0QH, UK
*Author for correspondence (simon.cook@bbsrc.ac.uk)

Accepted 11 November 2010
Journal of Cell Science 124, 969-977

doi:10.1242/jcs.058438

Summary

BIM-extra long (BIM_{EL}), a pro-apoptotic BH3-only protein and part of the BCL-2 family, is degraded by the proteasome following activation of the ERK1/2 signalling pathway. Although studies have demonstrated poly-ubiquitylation of BIM_{EL} in cells, the nature of the ubiquitin chain linkage has not been defined. Using ubiquitin-binding domains (UBDs) specific for defined ubiquitin chain linkages, we show that BIM_{EL} undergoes K48-linked poly-ubiquitylation at either of two lysine residues. Surprisingly, $BIM_{EL}\Delta KK$, which lacks both lysine residues, was not poly-ubiquitylated but still underwent ERK1/2-driven, proteasome-dependent turnover. BIM has been proposed to be an intrinsically disordered protein (IDP) and some IDPs can be degraded by uncapped 20S proteasomes in the absence of poly-ubiquitylation. We show that BIM_{EL} is degraded by isolated 20S proteasomes but that this is prevented when BIM_{EL} is bound to its pro-survival target protein MCL-1. Furthermore, knockdown of the proteasome cap component Rpn2 does not prevent BIM_{EL} turnover in cells, and inhibition of the E3 ubiquitin ligase β-TrCP, which catalyses poly-Ub of BIM_{EL}, causes Cdc25A accumulation but does not inhibit BIM_{EL} turnover. These results provide new insights into the regulation of BIM_{EL} by defining a novel ubiquitin-independent pathway for the proteasome-dependent destruction of this highly toxic protein.

Key words: BIM_{EL}, ERK1/2, Intrinsically disordered protein, 20S proteasome, Ubiquitin

Introduction

BIM (BCL2-interacting mediator of cell death), a pro-apoptotic, BH3-only protein belonging to the BCL-2 protein family plays an important role in promoting cell death in response to several stimuli (Bouillet et al., 1999). In particular, BIM-encoding mRNA and BIM protein levels increase upon growth factor withdrawal, and BIM promotes cell death under these conditions (Bouillet et al., 1999; Whitfield et al., 2001; Ewings et al., 2007). Among the common BIM splice variants (BIM-short, BIM-long and BIM-extra long) BIM-extra long (BIM_{EL}) is the most abundant and exhibits the most dynamic increases in expression following cytokine withdrawal (Whitfield et al., 2001; Weston et al., 2003; Ewings et al., 2007). Activation of the extracellular-signal-regulated kinases 1 and 2 (ERK1/2) pathway promotes the multisite phosphorylation of BIM_{EL}, resulting in its proteasome-dependent degradation (Ley et al., 2003; Luciano et al., 2003; Marani et al., 2004). *BIM* is a tumour suppressor gene (Egle et al., 2004) and stabilization of BIM_{EL} resulting from ERK1/2 inhibition is important in tumour cell death (Wickenden et al., 2008; Gillings et al., 2009). Consequently, understanding the mechanism of BIM_{EL} degradation is of fundamental interest and will inform the use of new oncogene-targeted therapeutics.

The identity of the E3 ubiquitin (Ub) ligase responsible for poly-ubiquitylation (poly-Ub) of BIM_{EL} has been controversial (Akiyama et al., 2003; El Chami et al., 2005; Wiggins et al., 2007; Zhang et al., 2008). However, a recent study has demonstrated that ERK1/2 and ribosomal S6 kinase (RSK) cooperate to phosphorylate BIM_{EL}, allowing binding of the F-box protein β-TrCP, which promotes BIM_{EL} poly-Ub (Dehan et al., 2009). Despite this, the nature of the Ub chain linkage that modifies BIM_{EL} in cells has never been defined. Here, we have used Ub-binding domains (UBDs) with defined selectivity for lysine 48 (K48)- or K63-linked Ub chains to show that BIM_{EL} is subject to K48-linked poly-Ub in cells following ERK1/2 activation. However, a BIM_{EL} mutant lacking lysine residues failed to undergo poly-Ub but was still degraded in a proteasome-dependent fashion. BIM_{EL} has been proposed to be an intrinsically disordered protein (IDP) (Hinds et al., 2007) and many IDPs can be degraded by uncapped 20S proteasomes without prior poly-Ub (Tsvetkov et al., 2008; Baugh et al., 2009). We now show that BIM_{EL} is degraded by 20S proteasomes in the absence of poly-Ub, but is protected from this by binding to the pro-survival BCL-2 protein, MCL-1. These results provide new insights into the regulation of BIM_{EL} by defining a novel, Ub-independent pathway for its destruction; consistent with this, we find that inhibition of cullin-based E3 ligases such as β-TrCP has no effect on BIM_{EL} abundance or turnover. Thus, cells employ multiple mechanisms to ensure the rapid destruction of this highly toxic protein.

Results

Use of immobilized UBDs to demonstrate that BIM_{EL} is modified by K48-linked poly-ubiquitin chains

Although K48-linked poly-Ub is recognized as a signal for degradation by the 26S proteasome, the nature of the Ub chain

linkage on BIM_{EL} has not been previously defined. Up to eight different types of Ub chain linkage might exist and this complexity is interpreted within cells by various UBDs, some of which have exquisite specificity for individual types of Ub chain linkage (Komander et al., 2009; Komander, 2009). To define the Ub chain linkage on BIM_{EL} we used the immobilized Ub-associated (UBA) domains of GST–Dsk2 and GST–Mud1, which specifically bind K48-linked Ub chains (Ohno et al., 2005; Trempe et al., 2005; Lowe et al., 2006; Komander et al., 2009), and the NZF domain of GST–Tab2c, which is specific for K63-linked chains (Kulathu et al., 2009).

GST–UBDs on GSH-agarose beads were used in a pulldown assay to capture and partially purify poly-Ub BIM constructs from cell extracts. We first confirmed the specificity of GST–Dsk2 and GST–Mud1 for K48-linked chains using antibodies specific for K48- or K63-linked poly-ubiquitin chains (Newton et al., 2008). HEK293 cells were transfected with empty vector or BIM_{EL}, and cell extracts were incubated with GST–Dsk2 UBA immobilized on GSH-agarose beads. These samples were readily detected by the K48-specific poly-ubiquitin antibody, which revealed a characteristic smear of poly-Ub species running up the gel, whereas the K63-specific poly-ubiquitin antibody failed to detect any material in the GST–Dsk2 pulldowns except the weak 'ghost' of the GST–Dsk2 protein itself, which is present in excess (Fig. 1A). The overexpression of BIM_{EL} made no difference to the pattern of K48-linked poly-Ub species, indicating that it represents a tiny fraction of the total K48-linked poly-ubiquitin in cells. When these same samples were blotted with antibodies to BIM, we could readily detect full-length BIM_{EL} and its poly-Ub species running as a smear up the gel in the sample from BIM_{EL}-transfected cells. We could also detect endogenous BIM_{EL} binding to GST–Dsk2 UBA, although the much lower levels meant that poly-Ub species of the endogenous BIM_{EL} were difficult to detect (Fig. 1A). Identical results were obtained when we used GST–Mud1 UBA to precipitate BIM_{EL} from control and transfected HEK293 cells (supplementary material Fig. S1A).

To define the specificity of the interaction between BIM_{EL} and GST–Dsk2 UBA, we performed several further experiments. First, it is known that activation of the ERK1/2 pathway promotes the phosphorylation and enhances the turnover of BIM_{EL} (Ley et al., 2003; Ewings et al., 2007). Consistent with this, when expressed in HR1 cells (HEK293 cells stably expressing the conditional kinase ΔRAF-1:ER*) (Ewings et al., 2007), the basal level of poly-Ub BIM_{EL}, detected by binding to GST–Dsk2, was greatly enhanced when BIM_{EL} phosphorylation was promoted by 4-hydroxytamoxifen (4-HT)-dependent activation of the ΔRAF-1:ER–MEK1/2–ERK1/2 pathway (Fig. 1B). Second, we compared BIM_{EL} binding to GST–Dsk2 with that of BIM_L and BIM_S (Fig. 1C), which lack the ERK1/2 and RSK phosphorylation sites that are thought to be the primary signal for poly-Ub and turnover. We again observed good binding of BIM_{EL}, and poly-Ub species were readily apparent. However, binding was very weak with BIM_L and particularly BIM_S and no poly-Ub species were detected (Fig. 1D), consistent with reports that BIM_L and BIM_S stability is not regulated by ERK1/2 (Luciano et al., 2003; Ley et al., 2004; Wickenden et al., 2008). We also observed that the binding of BIM_{EL} was drastically reduced when an inactive mutant form of GST–Dsk2 UBA was used in these pulldown experiments (Fig. 1D), and similar results were obtained with an inactive, mutant form of the GST–Mud1 UBA domain (supplementary material Fig. S1B). Finally, the GST–Tab2c NZF domain, which binds K63-linked poly-ubiquitin chains but not K48-linked chains (Kulathu et al., 2009), failed to precipitate poly-Ub BIM_{EL} whereas GST–Dsk2 was again effective (supplementary material Fig. S1C). Thus, using the K48 linkage specificity of the Dsk2 and Mud1 UBA domains we demonstrate for the first time that BIM_{EL} is subject to K48-linked poly-Ub in cells and this is enhanced following activation of the ERK1/2 pathway.

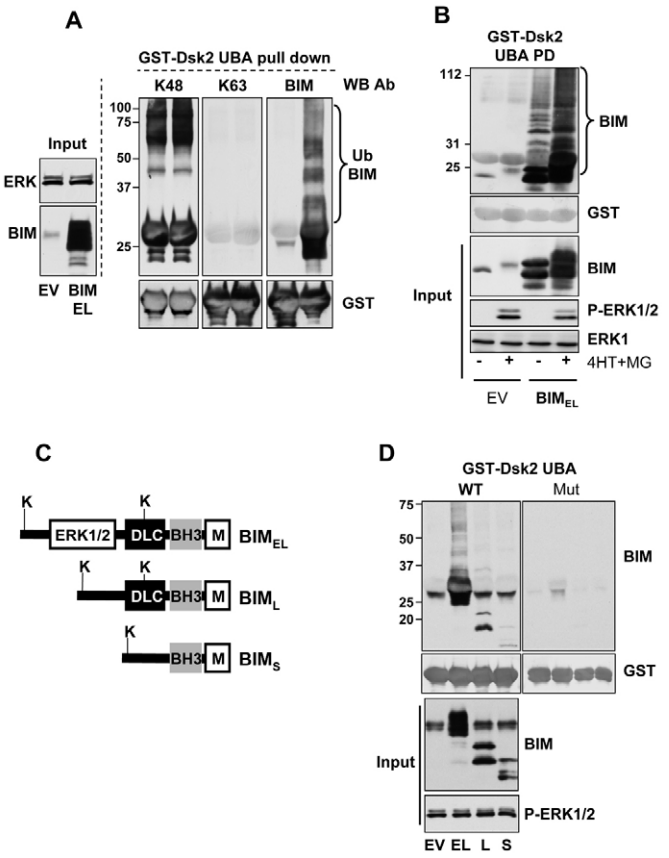

Fig. 1. Binding to the Dsk2 UBA domain demonstrates that BIM_{EL} undergoes K48-linked polyubiquitylation. (**A**) Cycling HEK293 cells were transfected with empty vector (EV) or pcDNA3–HA–BIM_{EL}. After 18 hours, cells extracts were precipitated with GST–Dsk2 UBA beads. Pulldowns were divided into three, fractionated by SDS-PAGE, and immunoblotted with antibodies specific for K48-linked Ub, K63-linked Ub, BIM or GST; the input samples were immunoblotted with antibodies for BIM or ERK1. (**B**) Cycling HR1 cells were transfected with empty vector (EV) or HA–BIM_{EL} for 16 hours before being switched to serum-free medium and treated with or without 100nM 4-HT + 10 μM MG132 for 1 hour. Whole cell lysates were generated and used for precipitation of poly-ubiquitylated protein using GST–Dsk2 UBA beads. Pulldowns were fractionated by SDS-PAGE and immunoblotted with antibodies specific for BIM or GST; the input samples were immunoblotted with antibodies for BIM, P-ERK1/2 or ERK1. (**C**) Representation of BIM_{EL}, BIM_L and BIM_S indicating the ERK1/2-responsive domain, DLC binding domain, BH3 domain, membrane binding motif (M) and the position of the two lysine residues, K3 and K108, numbered according to rat BIM_{EL}. (**D**) Cycling HEK293 cells were transfected with empty vector (EV) or pcDNA3 plasmids encoding HA–BIM_{EL}(EL), HA–BIM_L (L) or HA–BIM_S (S). After 18 hours, cells extracts were precipitated with wild-type or mutant GST–Dsk2 UBA beads. Pulldowns were fractionated by SDS-PAGE and immunoblotted with antibodies specific for BIM or GST; the input samples were immunoblotted with antibodies for BIM or P-ERK1/2.

BIM_{EL}ΔKK undergoes normal ERK1/2-driven proteasome-dependent turnover

Covalent attachment of Ub typically takes place at lysine residues. BIM_{EL} contains only two lysine residues at K3 and K108 (numbered according to the rat sequence) (Fig. 1C) so we mutated either K3 (BIM_{EL}ΔK) or K3 and K108 (BIM_{EL}ΔKK). These mutants were transfected into HR1 cells that were then treated with 4-HT+MG132 (Fig. 2A). Wild-type BIM_{EL} again exhibited a basal level of poly-Ub that was enhanced by 4-HT treatment. Mutation of K3 reduced the degree of basal and 4-HT-driven poly-Ub and caused the loss of certain poly-Ub species, whereas we failed to detect poly-Ub of BIM_{EL}ΔKK despite overexposure of the blots (Fig. 2A). Thus, poly-Ub can take place at both lysine residues in BIM_{EL} and mutation of both is required to generate a non-poly-Ub form.

Because BIM_{EL}ΔKK was not poly-Ub in cells, we anticipated that it would accumulate at higher levels and so elicit greater cell death than wild-type BIM_{EL}. However, we found that BIM_{EL} and BIM_{EL}ΔKK were equally effective at killing when transiently expressed in HEK293 cells (Fig. 2B). Furthermore, western blots revealed that wild-type BIM_{EL} and BIM_{EL}ΔKK were expressed at similar levels in transfected HR1 cells (Fig. 2A). These results prompted us to evaluate the turnover of the BIM_{EL}ΔKK protein directly. When HR1 cells were transfected in parallel with haemagglutinin (HA)–BIM_{EL} (Fig. 2C) or HA–BIM_{EL}ΔKK (Fig. 2D) the two proteins again expressed at similar levels and exhibited very similar turnover in response to activation of the ERK1/2 pathway by 4-HT (Fig. 2C,D). As a further control, we observed that the ΔRAF-1:ER*-driven turnover of both HA–BIM_{EL} and HA–BIM_{EL}ΔKK was inhibited when ERK1/2 activation was prevented by the MEK1/2 inhibitor U0126 (supplementary material Fig. S2A,B). Thus, both wild-type BIM_{EL} and BIM_{EL}ΔKK exhibited very similar ΔRAF-1:ER*-driven, MEK1/2-dependent turnover, despite BIM_{EL}ΔKK being defective for poly-Ub.

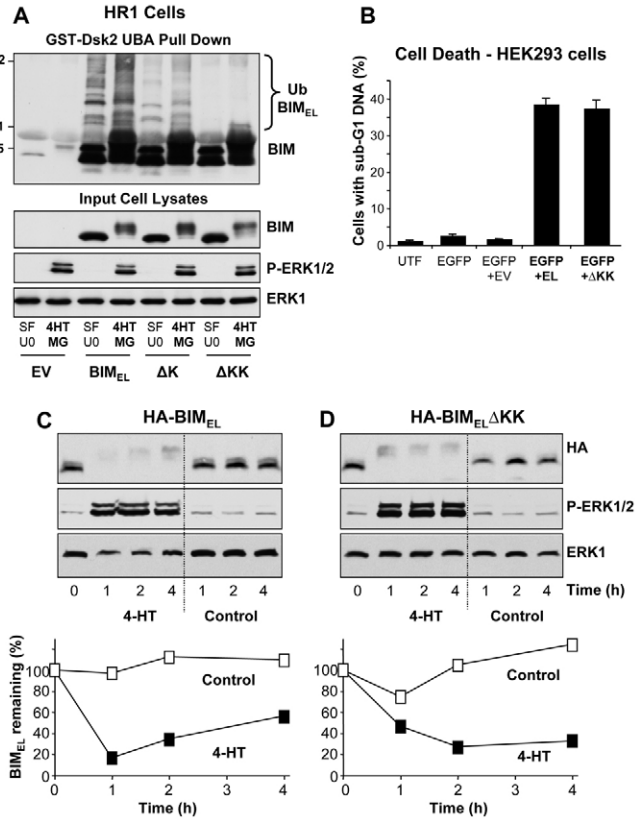

Fig. 2. Mutation of lysine residues within BIM_{EL} abolishes poly-Ub but does not prevent ERK1/2-dependent phosphorylation and degradation. (**A**) HR1 cells were transfected with HA–BIM_{EL}, HA–BIM_{EL}ΔK (K3R) or HA–BIM_{EL}ΔKK (K3R+K108R) for 16 hours. Cells were then treated with serum-free medium + 10 μM U0126 (SF U0) or 100 nM 4-HT + 10 μM MG132 (4HT MG) for one hour. Cells were harvested and poly-Ub proteins precipitated using GST–Dsk2 UBA. Input and precipitations were separated by SDS-PAGE and immunoblotted with antibodies to BIM, P-ERK1/2 and ERK1. (**B**) Cycling HR1 cells were co-transfected with empty vector (EV), HA–BIM_{EL} or HA–BIM_{EL}ΔKK in combination with EGFP-spectrin in a 5:1 ratio to allow the selection of BIM_{EL}-positive cells; UTF, untransfected. Cells were fixed and stained with propidium iodide, and the sub-G1 DNA content of GFP-positive cells measured by flow cytometry. Data is expressed as mean ± s.d. of triplicate cell replicates from a single experiment representative of three. (**C**,**D**) HR1 cells were transfected with HA–BIM_{EL} (C) or HA–BIM_{EL}ΔKK (D) for 16 hours before being switched to serum-free medium containing emetine. Cells were then treated with vehicle control (control) or 100 nM 4-HT for 1, 2 or 4 hours. Samples were prepared for BIM, P-ERK1/2 and ERK1/2 analysis by western blot. In each case, BIM_{EL} levels were quantified by densitometry, normalized to the loading control (ERK1), expressed as a percentage of BIM_{EL} present at time zero and represented graphically.

Proteasome-dependent degradation of BIM_{EL} in the absence of poly-Ub

In considering other pathways that might contribute to the rapid turnover of BIM_{EL} in the absence of poly-Ub we examined autophagy, a catabolic process in which the cell's own components are degraded by recruitment to autophagolysosomes. We compared immortalized mouse embryo fibroblasts (iMEFs) from wild-type and Atg5–/– mice (Kuma et al., 2004), which are defective for autophagy as judged by LC3 processing (Fig. 3A). The basal level of BIM_{EL} was higher in Atg5–/– iMEFs compared to wild-type cells, and Atg5–/– iMEFs also exhibited a more pronounced increase in BIM_{EL} compared to wild-type when the cells were serum starved (Fig. 3A). However, when we added cycloheximide, which both inhibits protein synthesis and activates ERK1/2, to serum-starved cells we found that the turnover of BIM_{EL} at 3 and 6 hours was essentially identical between the two cell types (Fig. 3A). These results suggest that autophagy might contribute to determining the basal level of BIM_{EL} but plays little or no role in acute ERK1/2-driven turnover of BIM_{EL}.

Since the first description (Ley et al., 2003), dozens of laboratories have shown that ERK1/2-driven turnover of BIM_{EL} is proteasome-dependent in a wide variety of cell types, as judged by the use of small molecule proteasome inhibitors including MG132, bortezomib (Velcade), and lactacystin. We used these same inhibitors to examine the acute turnover or long-term accumulation of HA–BIM_{EL}ΔKK. MG132 was able to effectively inhibit the ΔRAF-1:ER*-driven turnover of HA–BIM_{EL}ΔKK (Fig. 3B) and similar results were obtained with bortezomib (Fig. 3C). Furthermore, when cells were transfected with BIM_{EL} constructs and treated chronically with lactacystin, both BIM_{EL} and BIM_{EL}ΔKK proteins accumulated to the same degree and with the same kinetics (Fig. 3D). Together these results suggested the presence of an alternative poly-Ub-independent pathway for proteasome-dependent degradation of BIM_{EL}ΔKK following ERK1/2 activation.

BIM_{EL} and BIM_{EL}ΔKK are degraded by 20S proteasomes

A recent structural study reported that BIM is an IDP (Hinds et al., 2007), although the functional consequences of this were not

investigated. There is a growing appreciation that some disordered proteins can be degraded by uncapped 20S proteasomes independently of poly-Ub (Tsvetkov et al., 2008; Baugh et al., 2009); indeed, cleavage by the 20S proteasome has been proposed as an operational definition for IDPs (Tsvetkov et al., 2008). We used FoldIndex (Prilusky et al., 2005) to assess the distribution of folded and unfolded regions in BIM_{EL} using $p21^{CIP1}$ and PCNA (proliferating cell nuclear antigen) as comparators. This confirmed that $p21^{CIP1}$ was extensively unfolded (Kriwacki et al., 1996), whereas PCNA was almost exclusively folded (Fig. 4A), consistent with the PCNA crystal structure (Gulbis et al., 1996). In comparison, BIM_{EL} was largely unfolded, notably at the N-terminus and towards the C-terminus, though not including the C-terminal hydrophobic tail. Similar results were obtained when we used IUPred (Dosztanyi et al., 2005), to predict regions of disorder (supplementary material Fig. S3), confirming that BIM_{EL} is an IDP (Hinds et al., 2007).

Prompted by this, we investigated whether BIM_{EL} was degraded by 20S proteasomes. We first generated BIM_{EL} in vitro in a coupled transcription and translation (T&T) reaction and analysed the products using the GST–Dsk2 pulldown assay. Wild-type BIM_{EL} synthesized in vitro was poly-ubiquitylated and this was reduced in the $BIM_{EL}\Delta K$ mutant and abolished in the $BIM_{EL}\Delta KK$ mutant (Fig. 4B), reflecting previous observations in cells (Fig. 2A). To assess their degradation, [^{35}S]methionine-labelled BIM_{EL} or $BIM_{EL}\Delta KK$ were synthesized in the T&T reaction and incubated with purified 20S proteasomes. In common with $p21^{CIP1}$ (Touitou et al., 2001; Tsvetkov et al., 2008), both BIM_{EL} and $BIM_{EL}\Delta KK$ were rapidly degraded by 20S proteasomes whereas PCNA, a folded, globular protein was not (Fig. 4C). Thus, BIM_{EL} is an IDP

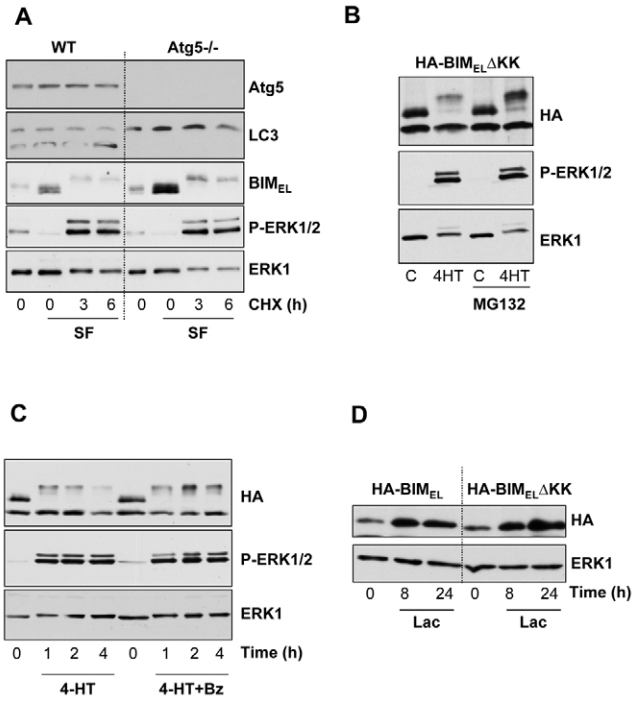

Fig. 3. HA–$BIM_{EL}\Delta KK$ undergoes ERK1/2-driven turnover via the proteasome. (**A**) Immortalized MEFs from wild-type (WT) or Atg5–/– mice were incubated in serum-free (SF) medium for 18 hours to induce BIM expression and then treated with cycloheximide (CHX) for 3 or 6 hours to inhibit protein synthesis and activate ERK1/2. Whole cell extracts were fractionated by SDS-PAGE and immunoblotted for Atg5, LC3, BIM, P-ERK1/2 and ERK1. (**B**) HR1 cells were transfected with HA–$BIM_{EL}\Delta KK$ for 16 hours and then switched to serum-free medium containing emetine and vehicle or 10 μM MG132 for 30 minutes prior to stimulation with 100 nM 4-HT for 2 hours. Controls (C) were not treated with 4-HT. Cells were harvested and samples immunoblotted with anti-HA (for $BIM_{EL}\Delta KK$), P-ERK1/2 or ERK1. (**C**) HR1 cells were transfected with HA–$BIM_{EL}\Delta KK$ for 16 hours and then switched to serum-free medium containing emetine and vehicle or 500 nM bortezomib (Bz) for 30 minutes prior to stimulation with 100 nM 4-HT for 1, 2 or 4 hours. Cells were harvested and samples immunoblotted with anti-HA (for $BIM_{EL}\Delta KK$), P-ERK1/2 or ERK1. (**D**) HR1 cells transfected with HA–BIM_{EL} or HA–$BIM_{EL}\Delta KK$ were treated with 0.5 μM lactacystin (Lac) and harvested after 8 or 24 hours for western blot analysis with the indicated antibodies.

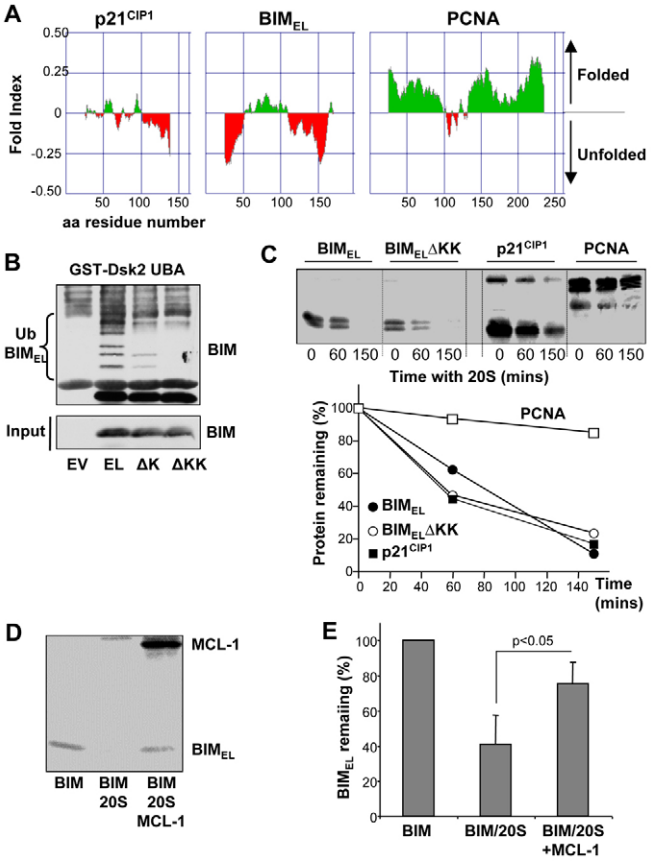

Fig. 4. BIM_{EL} is an intrinsically disordered protein that is degraded by the 20S proteasome in the absence of poly-Ub. (**A**) Plots generated using the FoldIndex algorithm (Prilusky et al., 2005) show the distribution of folded and unfolded regions for $p21^{CIP1}$, BIM_{EL} and PCNA. (**B**) Empty vector (EV), HA–BIM_{EL}, HA–$BIM_{EL}\Delta K$ and HA–$BIM_{EL}\Delta KK$ were processed through the in vitro T&T reaction and the resulting lysate used for precipitation of poly-Ub proteins using GST–Dsk2 UBA. (**C**) BIM_{EL}, $BIM_{EL}\Delta KK$, $p21^{CIP1}$ and PCNA were synthesized in vitro using a T&T reaction and [^{35}S]methionine; these proteins were then incubated with purified 20S proteasomes for the indicated time intervals, whereupon the degradation reaction was stopped, samples prepared for SDS-PAGE and detected by autoradiography. Quantification of this data is shown graphically, where the amount of protein is represented as a percentage of protein present at time zero. (**D**) BIM_{EL} and MCL-1 were synthesized in vitro using a T&T reaction and [^{35}S]methionine. BIM_{EL} was then incubated with purified 20S proteasomes with or without MCL-1. The degradation reaction was stopped, samples prepared for SDS-PAGE and detected by autoradiography. (**E**) Results quantified from three independent experiments in which BIM_{EL} was incubated with 20S proteasomes for 2 hours with or without MCL-1. *P<0.05, MCL-1 causes a statistically significant reduction in BIM_{EL} degradation by unpaired t-test.

that can be degraded by 20S proteasomes in the absence of poly-Ub.

One of the earliest consequences of ERK1/2-dependent phosphorylation of BIM_{EL} is promotion of its dissociation from pro-survival BCL-2 proteins such as MCL-1 or BCL-x_L (Ewings et al., 2007); indeed, the BIM_{EL}ΔBH3 mutant, with three point mutations in its BH3 domain, is defective for binding to MCL-1 or BCL-x_L and exhibits accelerated turnover in cells in the absence of ERK1/2 signalling (Ewings et al., 2007). Some IDPs are protected from 20S proteasomal degradation by interactions with their partner proteins (Alvarez-Castelao and Castaño, 2005; Tsvetkov et al., 2008) and, consistent with this, we observed that when incubated with recombinant MCL-1, recombinant HA–BIM_{EL} was protected from degradation by 20S proteasomes (Fig. 4D,E). This protection was not complete, but then it is likely that not all the MCL-1 protein produced in the T&T reaction was correctly folded to allow binding of all the BIM_{EL}. In addition, we noted that MCL-1 was itself partially degraded by 20S proteasomes (supplementary material Fig. S4A), consistent with recent reports (Stewart et al., 2010). Thus the effects of MCL-1 in this assay are probably an underestimate. The specificity of this effect was underlined by the demonstration that BIM_{EL}ΔBH3, which is defective for MCL-1 binding, was not protected by pre-incubation with recombinant MCL-1 (supplementary material Fig. S4B). Thus, binding of the BH3 domain of BIM_{EL} to one of its biological targets, MCL-1, protects it from degradation by 20S proteasomes.

Because activation of ERK1/2 can promote the poly-Ub of BIM_{EL} and its rapid turnover we speculated that Ub-dependent degradation by the 26S proteasome (UD/26S) and Ub-independent degradation by the 20S proteasome (UI/20S) pathways might operate in parallel, with the UD providing rapid and efficient targeting and the UI pathway serving as a failsafe, back-up pathway. Indeed, degradation of IDPs by the 20S proteasome has been described as ‘degradation by default’ (Asher et al., 2006; Tsvetkov et al., 2009b) and the fact the BIM_{EL}ΔKK turned over following ERK1/2 activation served as some support for this model. On the basis of this, we reasoned that inhibition of the UD/26S pathway might not prevent BIM_{EL} turnover. To test this we knocked down the Rpn2 subunit of the 19S proteasome cap to prevent the assembly of 26S proteasomes without affecting 20S proteasomes (Tsvetkov et al., 2009a). In cycling cells, knockdown of Rpn2 was effective and caused the accumulation of Cdc25A, a folded protein that is degraded by the UD/26S pathway (Fig. 5A); however, this had no effect on basal BIM_{EL} expression, suggesting the possibility of 26S-independent degradation. However, we were concerned that the low basal level of ERK1/2 and RSK activity in cycling HEK293 cells was not sufficient to provide a strong signal for BIM_{EL} turnover so that conditions were not optimal for observing any effects of Rpn2 knockdown. Instead, HR1 cells were transfected with RNAi oligonucleotides and subsequently stimulated with 4-HT to promote rapid BIM_{EL} turnover. Knockdown of Rpn2 caused some delay in the turnover of BIM_{EL} at early time points but ultimately did not prevent it, so that after 6 hours of stimulation the BIM_{EL} turnover was equal in both cell populations (Fig. 5B,C). Because BIM_{EL}ΔKK is turned over in a proteasome-dependent manner (Fig. 3) these results support the hypothesis that UD/26S and UI/20S pathways for BIM_{EL} turnover can operate in parallel, and that when the UD/26S pathway is inhibited BIM_{EL} turnover can still proceed by 20S-dependent degradation, albeit after a delay.

Inhibition of cullin-based E3 ligases has no effect on basal BIM_{EL} expression or ERK1/2-driven BIM_{EL} turnover

It has recently been shown that coordinated phosphorylation of BIM_{EL} by ERK1/2 and RSK provides a binding site for $SCF^{\beta\text{-TrCP1/2}}$, which promotes BIM_{EL} poly-Ub (Dehan et al., 2009). The Skp1/Cul1/F-box protein (SCF) complexes are perhaps the best-understood RING-type E3s (Cardozo and Pagano, 2004; Nakayama and Nakayama, 2006; Frescas and Pagano, 2008) and consist of a catalytic core (Cul1 and a RING protein) linked by an adaptor (SKP1) to a substrate-specific receptor subunit (the F-box protein). Recognition by F-box proteins often requires phosphorylation of the substrate, providing a link between signalling, poly-Ub and protein turnover. Examples of SCF complexes include SCF^{FBXW7}, which promotes the destruction of cyclin E (Koepp et al., 2001); SCF^{Skp2}, which promotes the destruction of $p21^{CIP1}$ and $p27^{KIP}$; and $SCF^{\beta\text{-TrCP1/2}}$, which promotes destruction IκB and Cdc25A (for a review, see Frescas and Pagano, 2008). If the UI/20S pathway could substitute for UD/26S, then we reasoned that disrupting BIM_{EL} poly-Ub by targeting its E3 ligase might not affect the levels of endogenous BIM_{EL}. To address this we inhibited cullin function using interfering mutants or RNAi-mediated knockdown of Cul1.

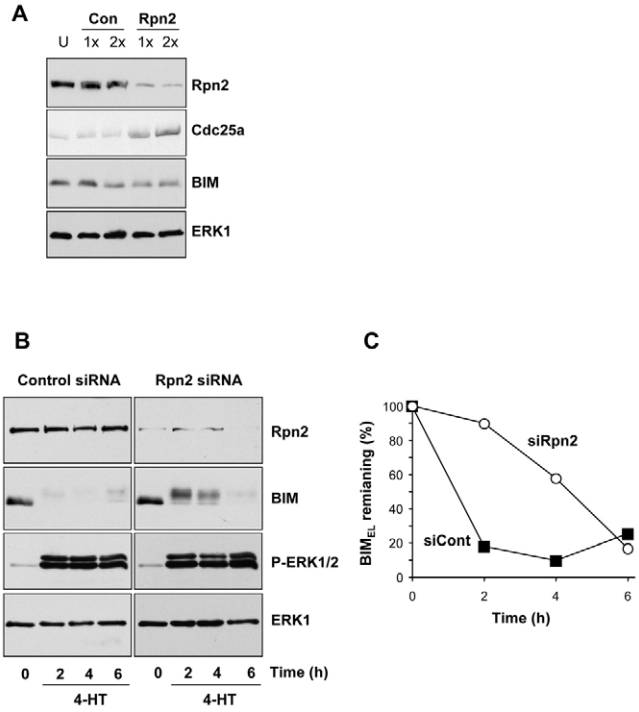

Fig. 5. Knockdown of the 19S cap component Rpn2 delays but does not prevent BIM_{EL} turnover. (**A**) HEK293 cells were subjected to one (1×) or two (2×) rounds of transfection with control (Con) or Rpn2-specific siRNA. Whole cell extracts were fractionated by SDS-PAGE and immunoblotted for Rpn2, Cdc25A, BIM or ERK1, which served as a loading control. (**B**,**C**) HR1 cells (HEK293+ΔRAF-1:ER*) were transfected with two rounds of control or Rpn2-specific siRNA. After 96 hours, cells were serum starved and stimulated with 4-HT for 2, 4 or 6 hours in the presence of emetine. (B) Whole cell extracts were fractionated by SDS-PAGE and immunoblotted for Rpn2, BIM, P-ERK1/2 or ERK1, which served as a loading control. (C) BIM_{EL} levels were quantified by densitometry, normalized to the loading control (ERK1), expressed as a percentage of BIM_{EL} present at time zero and represented graphically.

First, we expressed a dominant-negative interfering mutant of cullin1 (dnCul1) (Shirogane et al., 2005) in cycling HEK293 cells and examined the impact on basal protein expression. This approach was validated by showing that dnCul1 caused a substantial accumulation of $p27^{KIP1}$, cyclin E and Cdc25A, all of which are recognized SCF substrates (Fig. 6A); indeed, like BIM_{EL}, Cdc25A is a target of $SCF^{\beta\text{-}TrCP1/2}$ (for a review, see Frescas and Pagano, 2008). Despite this, dnCul1 did not cause an increase in the basal levels of BIM_{EL} (Fig. 6A). Because activation of ERK1/2 promotes BIM_{EL} turnover, we again reasoned that cycling cells were not optimal for BIM_{EL} turnover. As an alternative we again used HR1 cells, where activation of the ΔRAF-1:ER*–MEK1/2–ERK1/2 pathway results in a rapid and robust turnover of BIM_{EL} (Ewings et al., 2007). For these experiments we also used a dominant-negative mutant of Ubc12 (dnUbc12) (Amir et al., 2001), a protein that catalyses the NEDD8 conjugation of a conserved lysine residue that is required for the function of all cullins. The efficacy of dnUbc12 was validated by showing that it also caused accumulation of $p27^{KIP1}$ when expressed in cycling HEK293 cells, just like dnCul1 (Fig. 6B). Despite this, neither dnCul1 or dnUbc12 could block ΔRAF-1:ER*-driven turnover of BIM_{EL} (Fig. 6C). Finally, knockdown of Cul1 in HR1 cells by RNAi was also without effect on ΔRAF-1:ER*-driven turnover of BIM_{EL} (Fig. 6D).

These results revealed that selective inhibition of cullin1 (by two strategies) or inhibition of all cullins (using dnUbc12) failed to impair ERK1/2-dependent BIM_{EL} turnover. This data could suggest the existence of other E3 Ub ligases for BIM_{EL} in addition to $SCF^{\beta\text{-}TrCP1/2}$ (Dehan et al., 2009), but they are also consistent with our demonstration of an alternative Ub-independent pathway for BIM_{EL} degradation.

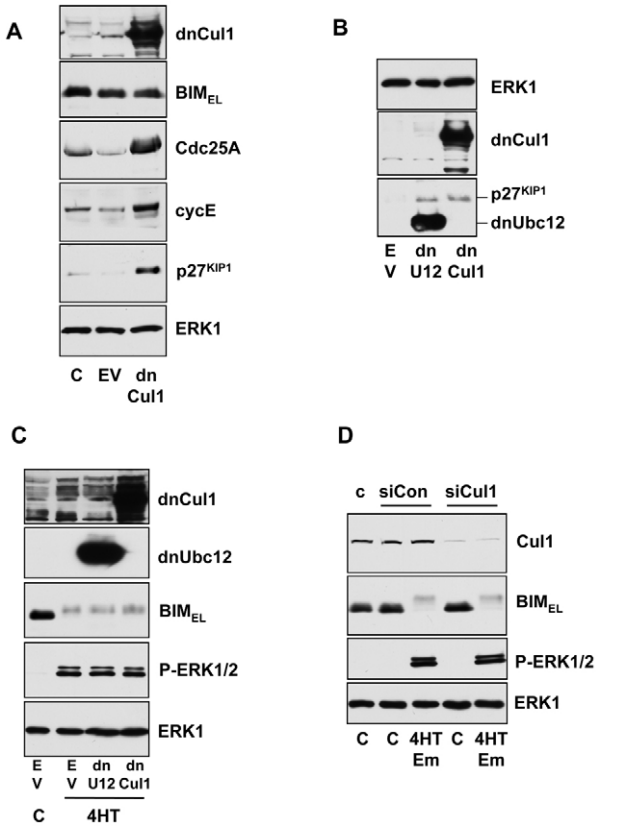

Fig. 6. Inhibition of cullin-based E3 ligases does not disrupt turnover of endogenous BIM_{EL}. (**A**) Cycling HEK293 cells were left untransfected (C) or transfected with empty vector (EV) or FLAG–dnCul1. After 24 hours, whole cell extracts were prepared, fractionated by SDS-PAGE and immunoblotted with antibodies to FLAG (dnCul1), BIM, Cdc25A, cyclin E (cycE) and $p27^{KIP1}$. (**B**) Cycling HEK293 cells were transfected with empty vector (EV), HIS–dnUbc12 or FLAG–dnCul1. After 24 hours, whole cell extracts were prepared, fractionated by SDS-PAGE and immunoblotted with antibodies to FLAG (dnCul1), HIS (dnUbc12) or $p27^{KIP1}$. (**C**) HR1 cells (HEK293+ΔRAF-1:ER*) were transfected with empty vector (EV), HIS–dnUbc12 or FLAG–dnCul1. After 24 hours, cells were stimulated with 4-HT + 10 μM emetine for 6 hours to activate the ERK1/2 pathway. Cell extracts were prepared, fractionated by SDS-PAGE and immunoblotted with antibodies to FLAG (dnCul1), HIS (dnUbc12) or BIM or P-ERK1/2. (**D**) HR1 cells were left untreated or transfected with control siRNA (siCon) or Cul1-specific siRNA (siCul1). Cells were then treated with 4-HT + 10 μM emetine for 8 hours or left untreated (C). Cell extracts were fractionated by SDS-PAGE and immunoblotted with antibodies to Cul1, BIM and P-ERK1/2. ERK1 served as a loading control in all experiments.

Discussion

Poly-Ub of a target protein determines the fate of that protein; K48-linked chains provide a signal for proteasomal degradation whereas K63-linked chains are important in the assembly of pro-inflammatory signalling complexes and protein trafficking (Ikeda and Dikic, 2008; Komander, 2009). The nature of the poly-ubiquitin chain linkage is typically defined by using individual Ub point mutants (K48R, K63R, etc.) to compete with endogenous Ub. However, such approaches have limitations (see Newton et al., 2008), require substantial overexpression of the mutant Ub (which can be difficult to achieve), and in our hands gave variable results. As an alternative we have made use of the ability of certain UBDs to discriminate between different Ub chain linkages (Komander et al., 2009). Such specificity underpins the use of ubiquitylation as a regulatory signal in a variety of cellular processes; however, in this instance we have used it simply as a diagnostic tool. The Dsk2 and Mud1 UBA domains have been defined as K48-specific by comparing their ability to bind chemically synthesized K48-linked, K63-linked and linear poly-Ub chains; similar studies have defined the K63 specificity of the TAB2C NZF domain (Kulathu et al., 2009). In addition, crystal structures have revealed the molecular basis by which the UBA domains from Dsk2 and Mud1 utilize the unique conformational features of K48-linked chains for specific recognition (Trempe et al., 2005; Lowe et al., 2006). Although the data are still at an early stage, emerging studies suggest that K11 linkages might be a second proteasomal degradation signal (Xu et al., 2009; Wu et al., 2010). K11-linked chains are compact and structurally distinct from K48-linked chains (Bremm et al., 2010) and neither Mud1 UBA or TAB2C NZF domains are able to interact with K11-linked poly-ubiquitin chains in pulldown experiments (Kulathu et al., 2009) (D.K., unpublished). Thus, the results of testing against all currently available Ub chain types strongly suggest that the Dsk2 and Mud1 UBA domains are specific for K48 chains, thereby validating our approach of using these UBA domains as diagnostic tools. Accordingly, our results demonstrate for the first time that BIM_{EL} is subject to K48-linked poly-Ub and define a simple assay for monitoring this linkage specificity in cells. We believe that such an assay might be more generally applicable to the study of K48-linked poly-Ub of proteins and are currently testing this.

Two pathways for ERK1/2-driven proteasomal degradation of BIM_{EL}

The ERK1/2 signalling pathway is the major pathway controlling the proteolytic turnover of BIM_{EL} (Ley et al., 2003) (for a review, see Gillings et al., 2009). Coordinated phosphorylation by ERK1/2 and RSK1/2 targets BIM_{EL} for poly-Ub by $SCF^{\beta\text{-}TrCP}$ (Dehan et al., 2009). Despite this, we found that a $BIM_{EL}\Delta KK$ mutant failed to undergo poly-Ub but was still subject to ERK1/2-driven, proteasome-dependent turnover. Prompted by the suggestion that BIM_{EL} is an IDP (Hinds et al., 2007), we found that BIM_{EL} (wild-type or ΔKK) could be degraded in a Ub-independent manner by 20S proteasomes. Further evidence for Ub-independent turnover of BIM_{EL} came from the demonstration that Rpn2 knockdown delayed, but did not prevent, BIM_{EL} turnover. Finally, inhibition of cullin-based E3 Ub ligases disrupted the turnover of $p27^{KIP1}$, cyclin E and Cdc25A (the latter a validated target of $SCF^{\beta\text{-}TrCP1/2}$) but had no effect on BIM_{EL} turnover. Taken together, these results provide strong, independent lines of evidence for an additional Ub-independent pathway for BIM_{EL} turnover by the proteasome.

We suggest that ERK1/2-driven degradation of BIM_{EL} proceeds by two pathways: classical Ub-dependent degradation by the 26S proteasome (UD/26S) or Ub-independent degradation by the 20S proteasome (UI/20S). In the former, phosphorylation of BIM_{EL} by ERK1/2 and RSK will allow the E3 ligase $SCF^{\beta TrCP}$ to promote the poly-Ub and 26S-dependent destruction of BIM_{EL} (Dehan et al., 2009). However, because ΔRAF-1:ER* can still promote the turnover of $BIM_{EL}\Delta KK$, it is apparent that ERK1/2 activation can also promote BIM_{EL} turnover by the proteasome, independently of poly-Ub. UI/20S degradation would explain why we could not prevent BIM_{EL} turnover by ΔKK mutation, Rpn2 knockdown or inhibition of cullin-based E3 ligases.

UI/20S is thought to be an important and evolutionarily conserved proteolytic pathway. Uncapped 20S proteasomes are abundant in mammalian cells and degrade up to 20% of cellular proteins (Baugh et al., 2009), including some proteins involved in cell cycle control and apoptosis. For example, the tumour suppressor p53 is degraded by a classical UD/26S mechanism but its N-terminus is disordered, allowing degradation by 20S proteasomes (Asher et al., 2005a; Asher et al., 2006; Tsvetkov et al., 2009a). Similarly, ornithine decarboxylase (Asher et al., 2005b), $p21^{CIP1}$ (Touitou et al., 2001) and IκBa (Krappmann et al., 1996; Alvarez-Castelao and Castaño, 2005) are all poly-Ub but can also be degraded by 20S. This default degradation pathway might serve as a back-up to ensure timely removal of these biologically important proteins (Asher et al., 2006).

BIM_{EL}, MCL-1 and the nanny model

We previously showed that phosphorylation of BIM_{EL} promotes its dissociation from pro-survival BCL-2 proteins; indeed, $BIM_{EL}\Delta BH3$, which is defective for binding to pro-survival BCL-2 proteins, is turned over more rapidly than wild-type BIM_{EL} suggesting that dissociation contributes to BIM_{EL} turnover (Ewings et al., 2007). Interestingly, some IDPs are protected from 20S degradation by interactions with their partner proteins (Alvarez-Castelao and Castaño, 2005; Tsvetkov et al., 2008; Tsvetkov et al., 2009a) and this has led to the suggestion that such partner proteins serve as 'nannies' (Tsvetkov et al., 2009b). Our demonstration that binding of BIM_{EL} to MCL-1 could protect it from degradation by 20S proteasomes (Fig. 4D,E) suggests that MCL-1 and presumably other pro-survival BCL-2 proteins serve as nannies for BIM_{EL}. In the course of writing up this work, a study reported that MCL-1 is degraded by 20S proteasomes in a Ub-independent manner (Stewart et al., 2010); the authors speculated that this was dependent on the disordered N-terminus of MCL-1. There are remarkable parallels with our study on BIM; both proteins are subject to poly-Ub and turnover by the UD/26S pathway but both proteins can also be degraded by the UI/20S pathway when poly-Ub is prevented by mutation of all lysine residues. Studies have previously shown that the binding of BH3-only proteins can influence MCL-1 stability in cells; Noxa binding promoted MCL-1 degradation (Willis et al., 2005), whereas binding of BIM (Czabotar et al., 2007) or PUMA (Mei et al., 2005) promoted MCL-1 stabilization. Although binding of BH3-only proteins could stabilize MCL-1 by displacing the E3 ligase MULE (Warr et al., 2005; Zhong et al., 2005), these new studies suggest an additional explanation whereby BIM_{EL} and MCL-1 serve as nannies for each other to prevent their degradation by 20S. The biological consequences of this are likely to be complex: dissociation of BIM_{EL} from MCL-1 (Ewings et al., 2007) would facilitate degradation of BIM_{EL}, which would support cell survival; conversely, this might also facilitate destruction of MCL-1 by the UD/26S or UI/20S pathways, which would tend to support cell death. The net effect is likely to be determined by the expression of other BCL-2 family proteins.

On the basis of these observations we propose that in addition to poly-Ub by β-TrCP (Dehan et al., 2009), phosphorylation-dependent dissociation from BCL-2 proteins represents a signal for targeting BIM_{EL} to the 20S proteasome. This might be because 'free' BIM_{EL} is intrinsically disordered or because dissociation of BIM_{EL} unmasks disordered regions or favours a disordered conformation that is a prerequisite for access to 20S proteasomes (Baugh et al., 2009). Phosphorylation of BIM_{EL} might contribute directly, because high net charge is often associated with disorder (Dyson and Wright, 2005). In this scenario, UD/26S would provide a rapid, targeted destruction mechanism, whereas the UI/20S pathway might operate to remove any excess or 'free' BIM_{EL} and serve as a 'failsafe' to ensure the removal of BIM_{EL} if ubiquitylation is disrupted. Quite how BIM_{EL} accesses the 20S proteasome remains to be seen. Non-Ub $p21^{CIP1}$ can bind to the REGγ 20S proteasome regulator (Li et al., 2007; Chen et al., 2007) or might be recognized by the C8α subunit of the 20S proteasome (Touitou et al., 2001). To date, we have not been able to detect specific binding of BIM_{EL} to C8α (M.J., C.M.W. and S.J.C., unpublished observations).

In summary we have used the inherent linkage specificity of the UBA domains of Dsk2 and Mud1 as a diagnostic tool to demonstrate that BIM_{EL} undergoes ERK1/2-driven, K48-linked poly-Ub. Despite this, poly-Ub is not a prerequisite for proteasomal degradation; we suggest that BIM_{EL} can also be degraded in a Ub-independent fashion by 20S proteasomes following its dissociation from pro-survival BCL-2 proteins, by virtue of its intrinsic disorder. These different mechanisms of degradation reflect the biological imperative of destroying BIM_{EL} in a timely fashion. BIM is one of the most toxic BH3-only proteins because of its ability to engage with all the pro-survival BCL-2 proteins (Chen et al., 2005). Consequently, its abundance must be tightly regulated by multiple mechanisms to ensure that cell death is only initiated under appropriate conditions.

Materials and Methods

Cells and cell culture

Culture of HR1 cells has been described previously (Ewings et al., 2007). SV40-immortalized MEFs from wild-type or Atg5–/– mice (Kuma et al., 2004), a kind gift

from Noboru Mizushima (Tokyo Medical and Dental University, Tokyo, Japan), were provided by Aviva Tolkovky (Universtiy of Cambridge, Cambridge, UK).

Antibodies

Antibodies that specifically recognize K48-linked or K63-linked Ub chains (Newton et al., 2008) were from Millipore. Other antibodies were obtained from the following vendors: cyclin E Ab-1 from Neomarkers; Cdc25A F6, cullin 1 D5 and anti-HA from Santa Cruz Biotechnology; $p27^{KIP1}$ Ab-2 from Calbiochem; BIM from Chemicon; phosphorylated ERK1/2 (P-ERK1/2) and ERK1/2 from Cell Signaling Technology; anti-His from Amersham Biosciences; and anti-FLAG from Sigma.

Constructs

His-tagged dominant-negative UBC12(C111S) in pcDNA3.1 was provided by Aaron Ciechanover (Technion, Haifa, Israel) (Amir et al., 2001). FLAG-tagged dominant-negative cullin 1 (dnCul1) was provided by Wade Harper (Harvard Medical School, Boston, MA) (Shirogane et al., 2005). The following UBD constructs were used: GST–Dsk2 UBA, wild-type (Ohno et al., 2005) and an inactive variant harbouring M342R and F344A point mutations; GST–Mud1 UBA, wild-type and the F330A mutant (Trempe et al., 2005); and GST–Tab2c NZF (Komander et al., 2009). GST–Dsk2 and GST–Mud1 fusions were expressed in DH5a cells, purified and immobilized on beads as described for GST–BIM (Ley et al., 2004). GST–Tab2c NZF (Komander et al., 2009) was expressed in BL21 cells and purified as described previously (Berrow et al., 2007). HA–BIM_{EL} (rat sequence) has been described previously (Ewings et al., 2007); K3R and/or K108R mutations in BIM_{EL} were introduced by site-directed mutagenesis.

Assay of BIM_{EL} poly-Ub in cells

HR1 cells were transfected with the indicated plasmids. After 24 hours, cells were serum starved in the presence of U0126 to inactivate ERK1/2 or treated with 4-HT + MG132 to activate ERK1/2 and inhibit the proteasome. Following lysis in TG lysis buffer (Ley et al., 2003) cell extracts were retained (input) or incubated end-over-end with immobilized GST–UBDs at 4°C for 2 hours, washed and fractionated by SDS-PAGE as described for GST–BIM pulldowns (Ley et al., 2004).

Assay of BIM_{EL} turnover in cells

HR1 cells were transfected with the indicated BIM_{EL} plasmids. After 24 hours, cells were treated with emetine to block new protein synthesis and chased in serum-free medium or in the presence or absence of 4-HT, U0126 or MG132. Cell extracts were fractionated by SDS-PAGE and immunoblotted as described.

In vitro translation

In vitro translation was performed using the T&T Quick Coupled Transcription/Translation System (Promega, Madison, WI). The plasmids employed were pCDNA3-BIM_{EL}, pCDNA3-BIM_{EL}ΔKK, pCDNA3-BIM_{EL}ΔBH3, pCDNA3-MCL-1, pIRES-$p21^{CIP1}$ and pIRES-PCNA.

In vitro 20S proteasomal degradation assay

Purified 20S proteasomes were generated as described previously (Asher et al., 2005b). [^{35}S]methionine-labelled proteins translated in vitro were incubated with 1 μg of purified 20S proteasomes in 150 mM NaCl, 50 mM Tris HCl, pH 7.5 at 37°C for the indicated times. Reactions were then resolved by SDS-PAGE, visualized by autoradiography and quantified by phosphorimaging (Tsvetkov et al., 2008).

RNAi against Cul1 and Rpn2

HR-1 cells (150,000 cells per well plated in a six-well plate) were plated in antibiotic-free media. Transfection complexes were prepared according to the manufacturer's instructions using Lipofectamine 2000 (Invitrogen). For Rpn2 knockdown, 200 pmol siRpn2-PT (5′-GCTCATATTGGGAATGCTTAT-3′) and 200 pmol siRpn2-MJ (5′-GGATACTTCTCCAGGATCA-3′) were mixed and 400 pmol of a control siRNA used (murine Bim1 5′-GGAGGAACCTGAAGATCTG-3′). Complexes were applied and cells incubated for 48 hours before being aspirated and fresh transfection complexes applied for a further 48 hours. Cells were then harvested immediately for western blot analysis, or an emetine chase experiment performed. For Cul1 knockdown, a pool of three siRNAs targeting Cul1 was used (Santa Cruz Biotechnology) alongside a human siRNA control (Santa Cruz Biotechnology). HR-1 cells were transfected for 24 hours, the transfection media was then aspirated and serum-free media applied. Following 16 hours of serum-free treatment, emetine (50 μM) was added to block protein synthesis followed 30 minutes later by addition of 4-HT for 8 hours.

We thank Rebecca Gilley and other members of the Cook laboratory for advice and encouragement and John Pascal (The Babraham Institute, Cambridge, UK) for initial advice on T&T reactions. We also thank Jane Endicott and Jean-Francois Trempe (University of Oxford, Oxford, UK), for providing the GST–Mud1 UBA constructs; Aaron Ciechanover, for dnUbc12 and J. Wade Harper, for dnCul1. This work was funded by core funding to the Babraham Institute and a response mode project grant from the BBSRC (BB/E02162X/1). C.M.W. was supported by a BBSRC PhD studentship and C.L.J. was supported by a BBSRC/AstraZeneca CASE studentship.

Supplementary material available online at
http://jcs.biologists.org/cgi/content/full/124/6/969/DC1

References

Akiyama, T., Bouillet, P., Miyazaki, T., Kadono, Y., Chikuda, H., Chung, U. I., Fukuda, A., Hikita, A., Seto, H., Okada, T. et al. (2003). Regulation of osteoclast apoptosis by ubiquitylation of proapoptotic BH3-only Bcl-2 family member Bim. *EMBO J.* **22**, 6653-6664.

Alvarez-Castelao, B. and Castaño, J. G. (2005). Mechanism of direct degradation of IkappaBalpha by 20S proteasome. *FEBS Lett.* **579**, 4797-4802.

Amir, R. E., Iwai, K. and Ciechanover, A. (2001). The NEDD8 pathway is essential for SCF(beta -TrCP)-mediated ubiquitination and processing of the NF-kappa B precursor p105. *J. Biol. Chem.* **277**, 23253-23259.

Asher, G., Tsvetkov, P., Kahana, C. and Shaul, Y. (2005a). A mechanism of ubiquitin-independent proteasomal degradation of the tumor suppressors p53 and p73. *Genes Dev.* **19**, 316-321.

Asher, G., Bercovich, Z., Tsvetkov, P., Shaul, Y. and Kahana, C. (2005b). 20S proteasomal degradation of ornithine decarboxylase is regulated by NQO1. *Mol. Cell* **17**, 645-655.

Asher, G., Reuven, N. and Shaul, Y. (2006). 20S proteasomes and protein degradation "by default". *Bioessays* **28**, 844-849.

Baugh, J. M., Viktorova, E. G. and Pilipenko, E. V. (2009). Proteasomes can degrade a significant proportion of cellular proteins independent of ubiquitination. *J. Mol. Biol.* **386**, 814-827.

Berrow, N. S., Alderton, D., Sainsbury, S., Nettleship, J., Assenberg, R., Rahman, N., Stuart, D. I. and Owens, R. J. (2007). A versatile ligation-independent cloning method suitable for high-throughput expression screening applications. *Nucleic Acids Res.* **35**, e45.

Bouillet, P., Metcalf, D., Huang, D. C., Tarlinton, D. M., Kay, T. W., Köntgen, F., Adams, J. M. and Strasser, A. (1999). Proapoptotic Bcl-2 relative Bim required for certain apoptotic responses, leukocyte homeostasis, and to preclude autoimmunity. *Science* **286**, 1735-1738.

Bremm, A., Freund, S. M. and Komander, D. (2010). Lys11-linked ubiquitin chains adopt compact conformations and are preferentially hydrolyzed by the deubiquitinase Cezanne. *Nat. Struct. Mol. Biol.* **17**, 939-947.

Cardozo, T. and Pagano, M. (2004). The SCF ubiquitin ligase: insights into a molecular machine. *Nat. Rev. Mol. Cell Biol.* **5**, 739-751.

Chen, L., Willis, S. N., Wei, A., Smith, B. J., Fletcher, J. I., Hinds, M. G., Colman, P. M., Day, C. L., Adams, J. M. and Huang, D. C. (2005). Differential targeting of prosurvival Bcl-2 proteins by their BH3-only ligands allows complementary apoptotic function. *Mol. Cell* **17**, 393-403.

Chen, X., Barton, L. F., Chi, Y., Clurman, B. E. and Roberts, J. M. (2007). Ubiquitin-independent degradation of cell-cycle inhibitors by the REGgamma proteasome. *Mol. Cell* **26**, 843-852.

Czabotar, P. E., Lee, E. F., van Delft, M. F., Day, C. L., Smith, B. J., Huang, D. C., Fairlie, W. D., Hinds, M. G. and Colman, P. M. (2007). Structural insights into the degradation of Mcl-1 induced by BH3 domains. *Proc. Natl. Acad. Sci. USA* **104**, 6217-6222.

Dehan, E., Bassermann, F., Guardavaccaro, D., Vasiliver-Shamis, G., Cohen, M., Lowes, K. N., Dustin, M., Huang, D. C., Taunton, J. and Pagano, M. (2009). betaTrCP- and Rsk1/2-mediated degradation of BimEL inhibits apoptosis. *Mol. Cell* **33**, 109-116.

Dosztányi, Z., Csizmok, V., Tompa, P. and Simon, I. (2005). IUPred: web server for the prediction of intrinsically unstructured regions of proteins based on estimated energy content. *Bioinformatics*. **21**, 3433-3434.

Dyson, H. J. and Wright, P. E. (2005). Intrinsically unstructured proteins and their functions. *Nat. Rev. Mol. Cell Biol.* **6**, 197-208.

Egle, A., Harris, A. W., Bouillet, P. and Cory, S. (2004). Bim is a suppressor of Myc-induced mouse B cell leukemia. *Proc. Natl. Acad. Sci. USA* **101**, 6164-6169.

El Chami, N., Ikhlef, F., Kaszas, K., Yakoub, S., Tabone, E., Siddeek, B., Cunha, S., Beaudoin, C., Morel, L., Benahmed, M. et al. (2005). Androgen-dependent apoptosis in male germ cells is regulated through the proto-oncoprotein Cbl. *J. Cell Biol.* **171**, 651-661.

Ewings, K. E., Hadfield-Moorhouse, K., Wiggins, C. M., Wickenden, J. A., Balmanno, K., Gilley, R., Degenhardt, K., White, E. and Cook, S. J. (2007). ERK1/2-dependent phosphorylation of BimEL promotes its rapid dissociation from Mcl-1 and Bcl-xL. *EMBO J.* **26**, 2856-2867.

Frescas, D. and Pagano, M. (2008). Deregulated proteolysis by the F-box proteins SKP2 and beta-TrCP: tipping the scales of cancer. *Nat. Rev. Cancer* **8**, 438-449.

Gillings, A. S., Balmanno, K., Wiggins, C. M., Johnson, M. and Cook, S. J. (2009). BIM as a mediator of tumour cell death in response to oncogene-targeted therapeutics. *FEBS J.* **276**, 6050-6062.

Gulbis, J. M., Kelman, Z., Hurwitz, J., O'Donnell, M. and Kuriyan, J. (1996). Structure of the C-terminal region of p21(WAF1/CIP1) complexed with human PCNA. *Cell* **87**, 297-306.

Hinds, M. G., Smits, C., Fredericks-Short, R., Risk, J. M., Bailey, M., Huang, D. C. and Day, C. L. (2007). Bim, Bad and Bmf: intrinsically unstructured BH3-only proteins that undergo a localized conformational change upon binding to prosurvival Bcl-2 targets. *Cell Death Differ.* **14**, 128-136.

Ikeda, F. and Dikic, I. (2008). Atypical ubiquitin chains: new molecular signals. 'Protein modifications: beyond the usual suspects' review series. *EMBO Rep.* **9**, 536-542.
Koepp, D. M., Schaefer, L. K., Ye, X., Keyomarsi, K., Chu, C., Harper, J. W. and Elledge, S. J. (2001). Phosphorylation-dependent ubiquitination of cyclin E by the SCFFbw7 ubiquitin ligase. *Science* **294**, 173-177.
Komander, D. (2009). The emerging complexity of protein ubiquitination. *Biochem. Soc. Trans*. **37**, 937-953.
Komander, D., Reyes-Turcu, F., Licchesi, J. D., Odenwaelder, P., Wilkinson, K. D. and Barford, D. (2009). Molecular discrimination of structurally equivalent Lys 63-linked and linear polyubiquitin chains. *EMBO Rep.* **10**, 466-473.
Krappmann, D., Wulczyn, F. G. and Scheidereit, C. (1996). Different mechanisms control signal-induced degradation and basal turnover of the NF-kappaB inhibitor IkappaB alpha in vivo. *EMBO J*. **15**, 6716-6726.
Kriwacki, R. W., Hengst, L., Tennant, L., Reed, S. I. and Wright, P. E. (1996). Structural studies of p21Waf1/Cip1/Sdi1 in the free and Cdk2-bound state: conformational disorder mediates binding diversity. *Proc. Natl. Acad. Sci. USA* **93**, 11504-11509.
Kulathu, Y., Akutsu, M., Bremm, A., Hofmann, K. and Komander, D. (2009). Two-sided ubiquitin binding explains specificity of the TAB2 NZF domain. *Nat. Struct. Mol. Biol*. **16**, 1328-1330.
Kuma, A., Hatano, M., Matsui, M., Yamamoto, A., Nakaya, H., Yoshimori, T., Ohsumi, Y., Tokuhisa, T. and Mizushima, N. (2004). The role of autophagy during the early neonatal starvation period. *Nature* **432**, 1032-1036.
Ley, R., Balmanno, K., Hadfield, K., Weston, C. and Cook, S. J. (2003). Activation of the ERK1/2 signaling pathway promotes phosphorylation and proteasome-dependent degradation of the BH3-only protein, Bim. *J. Biol. Chem*. **278**, 18811-18816.
Ley, R., Ewings, K. E., Hadfield, K., Howes, E., Balmanno, K. and Cook, S. J. (2004). Extracellular signal-regulated kinases 1/2 are serum-stimulated "Bim(EL) kinases" that bind to the BH3-only protein Bim(EL) causing its phosphorylation and turnover. *J. Biol. Chem*. **279**, 8837-8847.
Li, X., Amazit, L., Long, W., Lonard, D. M., Monaco, J. J. and O'Malley, B. W. (2007). Ubiquitin- and ATP-independent proteolytic turnover of p21 by the REGgamma-proteasome pathway. *Mol. Cell* **26**, 831-842.
Lowe, E. D., Hasan, N., Trempe, J. F., Fonso, L., Noble, M. E., Endicott, J. A., Johnson, L. N. and Brown, N. R. (2006). Structures of the Dsk2 UBL and UBA domains and their complex. *Acta. Crystallogr. D Biol. Crystallogr*. **62**, 177-188.
Luciano, F., Jacquel, A., Colosetti, P., Herrant, M., Cagnol, S., Pages, G. and Auberger, P. (2003). Phosphorylation of Bim-EL by Erk1/2 on serine 69 promotes its degradation via the proteasome pathway and regulates its proapoptotic function. *Oncogene* **22**, 6785-6793.
Marani, M., Hancock, D., Lopes, R., Tenev, T., Downward, J. and Lemoine, N. R. (2004). Role of Bim in the survival pathway induced by Raf in epithelial cells. *Oncogene* **23**, 2431-2441.
Mei, Y., Du, W., Yang, Y. and Wu, M. (2005). Puma(*)Mcl-1 interaction is not sufficient to prevent rapid degradation of Mcl-1. *Oncogene* **24**, 7224-7237.
Nakayama, K. I. and Nakayama, K. (2006). Ubiquitin ligases: cell-cycle control and cancer. *Nat. Rev. Cancer* **6**, 369-381.
Newton, K., Matsumoto, M. L., Wertz, I. E., Kirkpatrick, D. S., Lill, J. R., Tan, J., Dugger, D., Gordon, N., Sidhu, S. S., Fellouse, F. A. et al. (2008). Ubiquitin chain editing revealed by polyubiquitin linkage-specific antibodies. *Cell* **134**, 668-678.
Ohno, A., Jee, J., Fujiwara, K., Tenno, T., Goda, N., Tochio, H., Kobayashi, H., Hiroaki, H. and Shirakawa, M. (2005). Structure of the UBA domain of Dsk2p in complex with ubiquitin molecular determinants for ubiquitin recognition. *Structure* **13**, 521-532.
Prilusky, J., Felder, C. E., Zeev-Ben-Mordehai, T., Rydberg, E. H., Man, O., Beckmann, J. S., Silman, I. and Sussman, J. L. (2005). FoldIndex: a simple tool to predict whether a given protein sequence is intrinsically unfolded. *Bioinformatics* **21**, 3435-3438.
Shirogane, T., Jin, J., Ang, X. L. and Harper, J. W. (2005). SCFβ-TrCP controls clock-dependent transcription via casein kinase 1-dependent degradation of the mammalian period-1 (Per1) protein. *J. Biol. Chem*. **280**, 26863-26872.
Stewart, D. P., Koss, B., Bathina, M., Perciavalle, R. M., Bisanz, K. and Opferman, J. T. (2010). Ubiquitin-independent degradation of antiapoptotic MCL-1. *Mol. Cell. Biol*. **30**, 3099-3110.
Touitou, R., Richardson, J., Bose, S., Nakanishi, M., Rivett, J. and Allday, M. J. (2001). A degradation signal located in the C-terminus of p21WAF1/CIP1 is a binding site for the C8 alpha-subunit of the 20S proteasome. *EMBO J*. **20**, 2367-2375.
Trempe, J. F., Brown, N. R., Lowe, E. D., Gordon, C., Campbell, I. D., Noble, M. E. and Endicott, J. A. (2005). Mechanism of Lys48-linked polyubiquitin chain recognition by the Mud1 UBA domain. *EMBO J*. **24**, 3178-3189.
Tsvetkov, P., Asher. G., Paz, A., Reuven, N., Sussman, J. L., Silman, I. and Shaul, Y. (2008). Operational definition of intrinsically unstructured protein sequences based on susceptibility to the 20S proteasome. *Proteins* **70**, 1357-1366.
Tsvetkov, P., Reuven, N., Prives, C. and Shaul, Y. (2009a). Susceptibility of p53 unstructured N terminus to 20 S proteasomal degradation programs the stress response. *J. Biol. Chem*. **284**, 26234-26242.
Tsvetkov, P., Reuven, N. and Shaul, Y. (2009b). The nanny model for IDPs. *Nat. Chem. Biol*. **5**, 778-781.
Warr, M. R., Acoca, S., Liu, Z., Germain, M., Watson, M., Blanchette, M., Wing, S. S. and Shore, G. C. (2005). BH3-ligand regulates access of MCL-1 to its E3 ligase. *FEBS Lett*. **579**, 5603-5608.
Weston, C. R., Balmanno, K., Chalmers, C., Hadfield, K., Molton, S. A., Ley, R., Wagner, E. F. and Cook, S. J. (2003). Activation of ERK1/2 by ΔRaf-1:ER* represses Bim expression independently of the JNK or PI3K pathways. *Oncogene* **22**, 1281-1293.
Whitfield, J., Neame, S. J., Paquet, L., Bernard, O. and Ham, J. (2001). Dominant-negative c-Jun promotes neuronal survival by reducing BIM expression and inhibiting mitochondrial cytochrome c release. *Neuron* **29**, 629-643.
Wickenden, J. A., Jin, H., Johnson, M., Gillings, A. S., Newson, C., Austin, M., Chell, S. D., Balmanno, K., Pritchard, C. A. and Cook, S. J. (2008). Colorectal cancer cells with the BRAF(V600E) mutation are addicted to the ERK1/2 pathway for growth factor-independent survival and repression of BIM. *Oncogene* **27**, 7150-7161.
Wiggins, C. M., Band, H. and Cook, S. J. (2007). c-Cbl is not required for ERK1/2-dependent degradation of BimEL. *Cell. Signal.* **19**, 2605-2611.
Willis, S. N., Chen, L., Dewson, G., Wei, A., Naik, E., Fletcher, J. I., Adams, J. M. and Huang, D. C. (2005). Proapoptotic Bak is sequestered by Mcl-1 and Bcl-xL, but not Bcl-2, until displaced by BH3-only proteins. *Genes Dev*. **19**, 1294-1305.
Wu, T., Merbl, Y., Huo, Y., Gallop, J. L., Tzur, A. and Kirschner, M. W. (2010). UBE2S drives elongation of K11-linked ubiquitin chains by the anaphase-promoting complex. *Proc. Natl. Acad. Sci. USA* **107**, 1355-1360.
Xu, P., Duong, D. M., Seyfried, N. T., Cheng, D., Xie, Y., Robert, J., Rush, J., Hochstrasser, M., Finley, D. and Peng, J. (2009). Quantitative proteomics reveals the function of unconventional ubiquitin chains in proteasomal degradation. *Cell* **137**, 133-145.
Zhang, W., Cheng, G. Z., Gong, J., Hermanto, U., Zong, C. S., Chan, J., Cheng, J. Q. and Wang, L. H. (2008). RACK1 and CIS mediate the degradation of BimEL in cancer cells. *J. Biol. Chem*. **283**, 16416-16426.
Zhong, Q., Gao, W., Du, F. and Wang, X. (2005). Mule/ARF-BP1, a BH3-only E3 ubiquitin ligase, catalyzes the polyubiquitination of Mcl-1 and regulates apoptosis. *Cell* **121**, 1085-1095.